

RobNODDI: Robust NODDI Parameter Estimation with Adaptive Sampling under Continuous Representation

Taohui Xiao^{1,4}, Jian Cheng^{2,3}, Wenxin Fan⁴, Jing Yang⁴, Cheng Li⁴,
Enqing Dong¹, and Shanshan Wang^{4,5}

¹ School of Mechanical, Electrical & Information Engineering, Shandong University,
Weihai 264209, China

enqdong@sdu.edu.cn

² State Key Laboratory of Software Development Environment, Beihang University,
Beijing, China

³ Key Laboratory of Data Science and Intelligent Computing, Institute of
International Innovation, Beihang University, Hangzhou, Zhejiang, China

⁴ Paul C. Lauterbur Research Center for Biomedical Imaging, Shenzhen Institute of
Advanced Technology, Chinese Academy of Sciences, Shenzhen, Guangdong, China

ss.wang@siat.ac.cn

⁵ Peng Cheng Laboratory, Shenzhen, Guangdong, China

Abstract. Neurite Orientation Dispersion and Density Imaging (NODDI) is an important imaging technology used to evaluate the microstructure of brain tissue, which is of great significance for the discovery and treatment of various neurological diseases. Current deep learning-based methods perform parameter estimation through diffusion magnetic resonance imaging (dMRI) with a small number of diffusion gradients. These methods speed up parameter estimation and improve accuracy. However, the diffusion directions used by most existing deep learning models during testing needs to be strictly consistent with the diffusion directions during training. This results in poor generalization and robustness of deep learning models in dMRI parameter estimation. In this work, we verify for the first time that the parameter estimation performance of current mainstream methods will significantly decrease when the testing diffusion directions and the training diffusion directions are inconsistent. A robust NODDI parameter estimation method with adaptive sampling under continuous representation (RobNODDI) is proposed. Furthermore, long short-term memory (LSTM) units and fully connected layers are selected to learn continuous representation signals. To this end, we use a total of 100 subjects to conduct experiments based on the Human Connectome Project (HCP) dataset, of which 60 are used for training, 20 are used for validation, and 20 are used for testing. The test results indicate that RobNODDI improves the generalization performance and robustness of the deep learning model, enhancing the stability and flexibility of deep learning NODDI parameter estimation applications.

Keywords: Robustness · Diffusion MRI · Adaptive sampling · Continuous representation · NODDI parameter estimation

1 Introduction

Diffusion magnetic resonance imaging (dMRI) provides a unique tool for non-invasive assessment of tissue microstructure [1]. Neurite Orientation Dispersion and Density Imaging (NODDI) is a popular physiological component-based microstructural model in dMRI [2]. NODDI-derived measures can reflect changes in brain microstructural properties across a variety of neurological and psychiatric disorders, as well as brain development, maturation, and aging across the lifespan, including from neonatal to adolescence and adulthood [3,4,5,6,7].

Advanced dMRI models are highly nonlinear and composed of multiple compartments, so they often require dense sampling in q-space to better estimate parameters. Dense sampling in q-space requires the acquisition of many diffusion-weighted images (DWI) with different diffusion directions and b-value, which is very time-consuming and prone to motion artifacts [8]. In the current parameter estimation of advanced dMRI models, optimization-based methods such as nonlinear least squares (NLLS) method, the Markov chain Monte Carlo (MCMC) method, and Bayesian method are easy to produce estimation errors [1]. Moreover, deep learning-based methods have been widely used in microstructure estimation research [8,9,10,11,12,13,14,15,16,17,18,19,20]. Golkov et al. [9] used multilayer perceptron (MLP) for the first time to estimate diffusion kurtosis and microstructural parameters. Next various deep learning networks were used for dMRI model estimation. Chen et al. [10,17,18,19] proposed graph neural network (GNN) based structure to estimate the NODDI model parameters. Ye et al. [8,11,12,13] proposed a series of deep learning models to estimate NODDI model parameters. In addition, there are also studies [14,15,16] linking spherical harmonic (SH) coefficients to dMRI, among which Vishwesh et al. [16] directly used SH coefficients to estimate the microstructure. However, this study used images in the full gradient direction of single-shell, did not perform downsampling operations on single-shell, and did not fully exploit the multi-shell signal of dMRI. In summary, deep learning microstructure parameter estimation has achieved good results, speeding up parameter estimation and improving accuracy. However, the current testing process of deep learning models in microstructural parameter estimation needs to be highly consistent with training, that is, fixed DWI gradient direction information needs to be used. This results in poor generalization and clinical applicability of the deep learning model in dMRI microstructural parameter estimation, which does not meet the actual clinical needs.

To overcome these problems, in this article, we propose a robust adaptive sampling NODDI parameter estimation method under continuous representation (RobNODDI). We cut the original DWI into four-dimensional patches, then perform adaptive sampling, and then convert it into a continuous representation signal through SH fitting. Adaptive sampling can ensure that as much data as possible is involved in training, and the model can mine more useful information. Continuous representation helps the model be more flexible when testing diffusion directions and the training diffusion directions are inconsistent. These operations help our model achieve better results in random sampling tests. It is worth noting that our method has no special requirements for model architec-

ture and is theoretically suitable for most current mainstream models [21,22,23]. Therefore, we selected the advanced MESC-SD as our basic architecture [12].

In this study, our method was verified in the NODDI model. The dataset is the public the Human Connectome Project (HCP) dataset [24]. The results show that the proposed method can greatly improve the generalization and robustness of existing deep learning models, and has better clinical applicability.

2 Method

RobNODDI combines adaptive sampling and continuous representation. The purpose of adaptive sampling is to improve the network’s adaptability to different sampling data and fully mine and use the information in DWI. Continuous representation can make subsequent testing tasks more flexible by converting DWI into SH coefficients and allowing the model to directly learn this continuous representation. These strategies ensure that the diffusion directions of RobNODDI during testing does not need to be consistent with the diffusion directions during training, can effectively estimate parameter results, and significantly improve the generalization [25] and robustness of the deep learning model.

2.1 Overall Architecture

As shown in Figure 1, our method mainly has two core points: adaptive sampling and continuous representation. We first obtain DWI patches of a total of D diffusion directions for any two shells (b_i and b_j). During the training stage, we divide multi-shell into two independent shells and perform adaptive sampling respectively. A single shell can be sampled as $w \times w \times w \times N$, N represents the number of diffusion directions for adaptive sampling, which can be set between 20 and 60. Then the SH coefficients are calculated through linear least squares on the sampled patches, which is a continuously represented signal. Then we concatenate the SH coefficients of the two shells as input to the model for training. The size of the output parameter patch during training is generally set to be smaller than the input patch, and we set it to $(w-2) \times (w-2) \times (w-2) \times 3$. In the testing stage, we can accurately estimate the NODDI parameters by inputting DWI patches of two shells with sizes $w \times w \times w \times S_1$ and $w \times w \times w \times S_2$ respectively. Among them, S_1 and S_2 can be different from N in training, so RobNODDI will be more flexible and robust in clinical applications.

2.2 Continuous representation

The SH function is a special function defined on the sphere and has orthogonal completeness and continuity. It can be used as a set of orthogonal complete bases for functions on the sphere, and is used to expand and approximate functions on

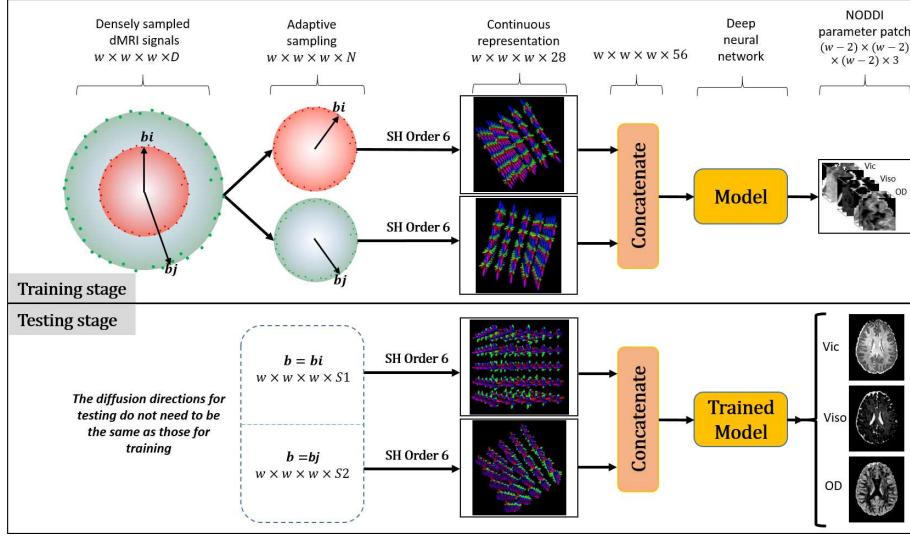


Fig. 1. Overview of RobNODDI. It contains training stage and testing stage. RobNODDI performs adaptive sampling and SH fitting on the DWI patches, and then concatenates the SH coefficients into the model. Note that both adaptive sampling and SH fitting are included in the training stage, and only SH fitting is included in the testing stage.

the sphere. Therefore, it is often used in dMRI [14,15,16,26,27]. The expansion formula of dMRI signal on the sphere is shown in formula (1).

$$D(\theta, \varphi) = \sum_{l=0}^{\infty} \sum_{m=-l}^l \hat{C}_l^m Y_l^m(\theta, \varphi) \quad (1)$$

Here, $D(\theta, \varphi)$ represents the normalized dMRI signal, \hat{C}_l^m represents the SH coefficient of dMRI, $Y_l^m(\theta, \varphi)$ represents the SH basis. l and m represent SH order and degree respectively. In dMRI, the direction of the diffusion gradient is described by θ, φ . Where θ and φ respectively represent two angles in the spherical coordinate system, namely the polar angle and the azimuth angle. When the basis is formed, the SH coefficients \hat{C}_l^m can be solved by regularized linear least squares fitting [14]. In practical applications, with the original DWI data and corresponding direction coordinate information, we can obtain the corresponding SH coefficients by solving formula (1).

2.3 Adaptive sampling

When sampling DWI signal in dMRI microstructure parameter estimation, uniform sampling is generally performed in q-space [11,26,27,28], which ensures a more balanced use of the information in DWI. But for deep learning models, the sampling of the model during testing must be consistent with the training, which is inflexible and leads to a greatly reduced generalization and robustness

of the model. Therefore, in this study, RobNODDI utilizes a combination of adaptive sampling and continuous representation. Specifically, each DWI patch used for training is randomly sampled, and the sampling pattern varies across different training epochs. Then, we perform Spherical Harmonics (SH) fitting on the adaptively sampled DWI patch, and finally input the processed patch into the network for training. In actual implementation, We first cut the DWI of the original two b values into $w \times w \times w \times D$, where the fourth dimension D represents all directions of the two arbitrary b values. Then we randomly sample the patches of the two shells separately to obtain patches of size $w \times w \times w \times N$, where N can be set between 20 and 60. We perform random sampling for each patch to enable the network to achieve adaptive sampling. After training on patches containing N diffusion directions, our model can be tested in multi-shell using S directions per shell that are different from the trained directions. In theory, it has better robustness than existing deep learning methods.

2.4 Network Construction

Our proposed method is independent of the network architecture used. Therefore, in this study, we utilize the MESC-SD developed for NODDI used in the study [12] as the basic architecture. The network architecture adopts SD-LSTM in the first step, which is constructed by unfolding an iterative process for solving the sparse reconstruction problem, and in the second stage by adding a fully connected layer to calculate the mapping of SH coefficient representations to NODDI parameter.

3 Experiments

In this section, we evaluate the proposed method to estimate NODDI parameters, including intracellular volume fraction (V_{icvf}), isotropic volume fraction (V_{iso}), and directional dispersion (OD) [2,12]. The network generalization performance is compared with deep learning methods such as q-DL [9], GCNN [10] and MESC-SD [12] through SS and RS tests. In particular, we use SS to indicate that the same sampling scheme is used during both testing and training. On the other hand, RS is used to indicate that random sampling is employed during testing, where the diffusion directions in the testing set are different from those used in the training set.

3.1 Implementation Details

We used 6-order SH (28 coefficients) in the HCP dataset, with $N=30$ diffusion directions for each shell, and select two shells of $b=1000$ s/mm² and $b=2000$ s/mm². We set $w=5$, which means cutting the patch into a size of $5 \times 5 \times 5 \times 180$, and the corresponding patch size of the NODDI parameter is $3 \times 3 \times 3 \times 3$. Additionally, mean square error (MSE) is used as the loss function and Adam is used as the optimizer. The initial learning rate and update method of different

experiments are different. The initial learning rate is mainly set to 0.0005 and 0.0001. The training epochs are 30 or 50, and the batchsize of all experiments is set to 128. All models are applied in pytorch2.0 and trained on a server equipped with TITAN Xp GPU.

3.2 Dataset and Evaluation Metrics

Dataset. We selected data from HCP dataset [21] to conduct experiments and test the results. The data set contains 3 b values (b=1000, 2000, 3000 s/mm²), 90 diffusion directions for each b value, and an additional 18 non-diffusion weighted volumes. We randomly selected 100 adult subjects and used 60% of them for training, 20% for validation, and the remaining 20% for testing. We obtain the gold standard by fitting all spherical shells with all gradient directions through AMICO [29].

Evaluation Metrics. We use the root mean square error (MSE), peak signal-to-noise ratio (PSNR), and structural similarity index measure (SSIM) to evaluate the quality of the predicted NODDI-derived indices.

3.3 Results

The whole experiment includes: Testing the poor generalization of current deep learning methods in parameter estimation under different diffusion directions. Evaluating whether fitting DWI with SH as input can help improve the generalization of existing methods. Demonstrating that the proposed RobNODDI method achieves the best robustness while ensuring good performance.

Table 1. Average quantitative indicators of NODDI parameters for SS and RS testing using different methods on the q-space data with 30 diffusion directions per shell (1000, 2000 s/mm²).

Method	Sampling in testing	MSE	PSNR	SSIM
q-DL [9]	SS	0.00463	23.41919	0.92024
	RS	0.00851	20.74516	0.88076
GCNN [10]	SS	0.00405	23.97635	0.92708
	RS	0.01268	19.00210	0.86630
MESCS-SD [12]	SS	0.00219	26.64520	0.95775
	RS	0.00842	20.79057	0.89852
MESCS-SD with SH	SS	0.00226	26.49617	0.95626
	RS	0.00263	25.82884	0.94980
RobNODDI	SS	0.00211	26.80304	0.95901
	RS	0.00211	26.79317	0.95884

SS and RS tests of existing deep learning methods. Table 1 shows the quantitative metrics of three deep learning methods under SS and RS testing. It can be observed that the existing deep learning methods suffer a significant performance drop when the diffusion direction changes, making it difficult to estimate the parameters accurately. The visual comparison in Figure 2 also demonstrates that the existing deep learning methods exhibit a clear performance degradation when the testing diffusion direction is altered. In other words, most existing deep learning methods have poor generalization to changes in dMRI diffusion direction.

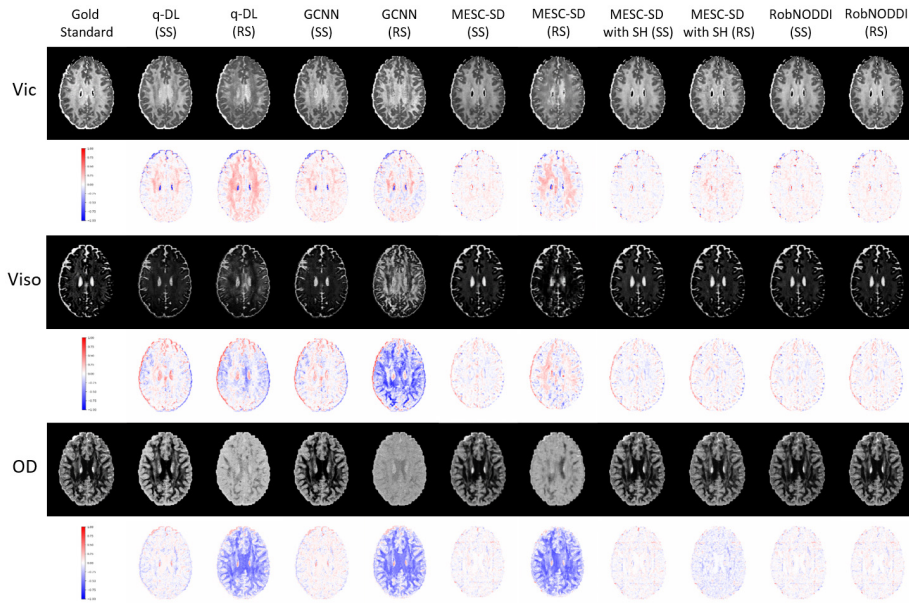


Fig. 2. Qualitative comparison of NODDI parameter for SS and RS testing using different methods with 30 diffusion directions per shell (1000, 2000 s/mm^2)

SS and RS testing using SH coefficients as input. The input for training here is the SH coefficient of 30 diffusion directions with fixed uniform sampling per shell. The test is also divided into two types: SS and RS. The results are shown in Figure 2 and Table 1 corresponding to MESC-SD with SH (SS) and MESC-SD with SH (RS). It can be seen that using SH as input to estimate microstructure parameters is effective, and the results are very close to using DWI as input. When the test direction is RS, the performance also decreases; however, compared to the original MESC-SD, the RS test shows much better results. This indicates that using continuous representation of DWI as input improves

the model’s generalization performance in dMRI microstructure parameter estimation, yet it still lags behind the SS test. Specifically, for Vic and OD, the visual results and error maps in Figure 2 still show some discrepancy compared to the SS testing results.

SS and RS test of the proposed RobNODDI method. This part introduces our proposed RobNODDI method. As shown in Figure 1, our input is the DWI patch, and we incorporate adaptive sampling and SH coefficient fitting into the network training. During testing, we also conducted SS and RS evaluations for RobNODDI, where the SS testing uses the same sampling scheme as the comparative methods. The corresponding results are shown in Figure 2 and Table 1. It can be observed that when the testing direction changes, the results estimated by our method remain highly consistent, with almost no visible differences, and the quantitative metrics are very close as well. Compared to the original MESC-SD method, our approach achieves significantly improved generalization. Moreover, compared to MESC-SD with SH, the proposed method further enhances both performance and generalization. Therefore, our method not only achieves more accurate parameter estimation, but also demonstrates strong generalization and robustness.

3.4 Ablation Study

Table 2. RobNODDI performs RS test of NODDI parameters on q-space data with different number of diffusion directions (1000, 2000 s/mm²)

Method	Sampling in testing	Number of directions	MSE	PSNR	SSIM
RobNODDI	RS	20/20	0.00231	26.40777	0.95512
		25/25	0.00217	26.67221	0.95759
		30/30	0.00211	26.80304	0.95901
		35/35	0.00208	26.85303	0.95952
		40/40	0.00208	26.87385	0.95989
		16/29	0.00226	26.50507	0.95590
		21/28	0.00219	26.64630	0.95730
		26/23	0.00219	26.64381	0.95732

RS test of RobNODDI method with different number of samples. To further validate the robustness of the proposed method, we conducted ablation experiments on RobNODDI by randomly sampling DWI with varying diffusion directions and numbers. This included tests with consistent numbers of diffusion directions for two b values: 40, 50, 70, and 80 directions (20, 25, 35 and 40 for b = 1000 s/mm² and b = 2000 s/mm²). And tests with different numbers of diffusion directions for two b values: 45, 49, and 49 directions (16, 21 and 26 for b = 1000 s/mm²; 29, 28 and 23 for b = 2000 s/mm²). The ablation results are presented in Table 2, highlighting the robustness of RobNODDI.

It is evident that performance slightly improves with an increasing number of diffusion directions used in testing. Moreover, our method consistently maintains stable performance and high flexibility across different numbers of DWI signals used for testing.

4 Conclusion and Future Work

In this work, we propose RobNODDI, which achieves robust NODDI parameter evaluation by combining adaptive sampling and continuous representation. By comparing with the existing deep learning microstructure estimation methods, it is shown that converting dMRI images into SH coefficients helps to improve the generalization of the original method for diffusion directions. The proposed RobNODDI can further improve the robustness and stability of the deep learning model in dMRI microstructure parameter estimation, making the deep learning model more flexible and universal in dMRI clinical applications. Moreover, the model architecture in the method does not rely on a specific network structure. In our future work, we will explore more advanced methods, such as [15,30], and further optimize the proposed approach.

Acknowledgement. This research was partly supported by the National Natural Science Foundation of China (62222118, U22A2040, 62171261, 81671848, 81371635), Guangdong Provincial Key Laboratory of Artificial Intelligence in Medical Image Analysis and Application (2022B1212010011), Shenzhen Science and Technology Program (RCYX20210706092104034, JCYJ20220531100213029), Key Laboratory for Magnetic Resonance and Multimodality Imaging of Guangdong Province (2023B1212060052), Youth Innovation Promotion Association CAS, National Key R&D Program of China (2023YFA1011400), Fundamental Research Funds for the Central Universities (China), and Innovation Ability Improvement Project of Science and Technology Small and Medium-sized Enterprises of Shandong Province (2021TSGC1028).

References

1. Johansen-Berg, H., Behrens, T. E.: Diffusion MRI: from quantitative measurement to in vivo neuroanatomy. Academic Press (2016)
2. Zhang, H., Schneider, T., Wheeler-Kingshott, C. A., et al.: NODDI: practical in vivo neurite orientation dispersion and density imaging of the human brain. *Neuroimage* **61**(4), 1000–1016 (2012)
3. Greenspan, H., Van Ginneken, B., Summers, R. M.: Guest editorial deep learning in medical imaging: Overview and future promise of an exciting new technique. *IEEE transactions on medical imaging* **35**(5), 1153–1159 (2016)
4. Fu, X., Shrestha, S., Sun, M., et al.: Microstructural white matter alterations in mild cognitive impairment and Alzheimer’s disease: study based on neurite orientation dispersion and density imaging (NODDI). *Clinical Neuroradiology* **30**, 569–579 (2020)

5. Kunz, N., Zhang, H., Vasung, L., et al.: Assessing white matter microstructure of the newborn with multi-shell diffusion MRI and biophysical compartment models. *Neuroimage* **96**, 288–299 (2012)
6. Mah, A., Geeraert, B., Lebel, C.: Detailing neuroanatomical development in late childhood and early adolescence using NODDI. *PLoS One* **12**(8), e0182340 (2017)
7. Billiet, T., Vandenbulcke, M., Madler, B., et al.: Age-related microstructural differences quantified using myelin water imaging and advanced diffusion MRI. *Neurobiology of aging* **36**(6), 2107–2121 (2015)
8. Zheng, T., Zheng, W., Sun, Y., et al.: An Adaptive Network with Extragradient for Diffusion MRI-Based Microstructure Estimation. In: Wang L. W., Dou Q., Fletcher P. T., Speidel S., Li S. (eds.) *MICCAI 2022*, LNCS, vol.13431, pp.153–162. Springer, Cham (2022). https://doi.org/10.1007/978-3-031-16431-6_15
9. Golkov, V., Dosovitskiy, A., Sperl, J. I., et al.: Q-space deep learning: twelve-fold shorter and model-free diffusion MRI scans. *IEEE transactions on medical imaging* **35**(5), 1344–1351 (2016)
10. Chen, G., Hong, Y., Zhang, Y., et al.: Estimating tissue microstructure with under-sampled diffusion data via graph convolutional neural networks. In: Martel A. L., Abolmaesumi P., Stoyanov D., Mateus D., Zuluaga M. A., Zhou S. K., Racoceanu D., Joskowicz L. (eds.) *MICCAI 2020*, LNCS, vol.12267, pp.280–290. Springer, Cham (2020). https://doi.org/10.1007/978-3-030-59728-3_28
11. Ye, C., Li, X., Chen, J.: A deep network for tissue microstructure estimation using modified LSTM units. *Medical image analysis*, **55**, 49–64 (2019)
12. Ye, C., Li, Y., Zeng, X.: An improved deep network for tissue microstructure estimation with uncertainty quantification. *Medical image analysis*, **61**, 101650 (2020)
13. Zheng, T., Yan, G., Li, H., et al.: A microstructure estimation Transformer inspired by sparse representation for diffusion MRI. *Medical Image Analysis*, **86**, 102788 (2023)
14. Koppers, S., Bloy, L., Berman, J.I., Tax, C.M.W., Edgar, J.C., Merhof, D. (2019). Spherical Harmonic Residual Network for Diffusion Signal Harmonization. In: Bonet-Carne, E., Grussu, F., Ning, L., Sepelband, F., Tax, C. (eds.) *Computational Diffusion MRI. MICCAI Workshop 2019. Mathematics and Visualization*. pp.173–182. Springer, Cham (2019). https://doi.org/10.1007/978-3-030-05831-9_14
15. Sedlar, S., Alimi, A., Papadopoulou, T., Deriche, R., Deslauriers-Gauthier, S.: A Spherical Convolutional Neural Network for White Matter Structure Imaging via dMRI. In: de Bruijne, M., et al. (eds.) *MICCAI 2021*. LNCS, vol.12903, pp.529–539. Springer, Cham (2021). https://doi.org/10.1007/978-3-030-87199-4_50
16. Nath, V., et al.: DW-MRI Microstructure Model of Models Captured Via Single-Shell Bottleneck Deep Learning. In: Gyori, N., Hutter, J., Nath, V., Palombo, M., Pizzolato, M., Zhang, F. (eds.) *Computational Diffusion MRI. MICCAI Workshop 2019. Mathematics and Visualization*. pp.147–157. Springer, Cham (2021). https://doi.org/10.1007/978-3-030-73018-5_12
17. Yang, J., et al.: Towards Accurate Microstructure Estimation via 3D Hybrid Graph Transformer. In: Greenspan, H., et al (eds.) *MICCAI 2023*. LNCS, vol. 14227, pp.25–34. Springer, Cham (2023). https://doi.org/10.1007/978-3-031-43993-3_3
18. Chen, G., et al.: Hybrid Graph Transformer for Tissue Microstructure Estimation with Undersampled Diffusion MRI Data. In: Wang, L., Dou, Q., Fletcher, P.T., Speidel, S., Li, S. (eds) *MICCAI 2022*. LNCS, vol 13431, pp.113–122. Springer, Cham (2022). https://doi.org/10.1007/978-3-031-16431-6_11
19. Chen, G., Hong Y., Huynh, K. M., et al.: Deep learning prediction of diffusion MRI data with microstructure-sensitive loss functions. *Medical image analysis*, **85**, 102742 (2023)

20. Gibbons, E. K., Hodgson, K. K., Chaudhari, A. S., et al.: Simultaneous NODDI and GFA parameter map generation from subsampled q-space imaging using deep learning. *Magnetic resonance in medicine*, **81**(4), 2399-2411 (2019)
21. Wang, S., Wu, R., Jia, S., et al.: Knowledge-driven deep learning for fast MR imaging: Undersampled MR image reconstruction from supervised to un-supervised learning. *Magnetic Resonance in Medicine*, **92**(2), 496-518 (2024)
22. Wang, S., Xiao, T., Liu, Q., Zheng, H.: Deep learning for fast MR imaging: A review for learning reconstruction from incomplete k-space data. *Biomedical Signal Processing and Control*, **68**, 102579 (2021)
23. Wang, S., Wu, R., Li, C.: Parcel: physics-based unsupervised contrastive representation learning for multi-coil mr imaging. *IEEE/ACM Transactions on Computational Biology and Bioinformatics*, **20**(5), 2659-2670 (2022)
24. Van Essen, D. C., Smith, S. M., Barch, D. M., et al.: The WU-Minn human connectome project: an overview. *Neuroimage*, **80**, 62-79 (2013)
25. Wu, R., Li, C., Zou, J., et al.: Generalizable Reconstruction for Accelerating MR Imaging via Federated Learning with Neural Architecture Search. *IEEE Transactions on Medical Imaging* (2024)
26. Caruyer, E., Lenglet, C., Sapiro, G., et al.: Design of multishell sampling schemes with uniform coverage in diffusion MRI. *Magnetic resonance in medicine*, **69**(6), 1534-1540 (2013)
27. Cheng, J., Shen, D., Yap, P.T.: Designing Single- and Multiple-Shell Sampling Schemes for Diffusion MRI Using Spherical Code. In: Golland, P., Hata, N., Barillot, C., Hornegger, J., Howe, R. (eds.) *MICCAI 2014*. LNCS, vol. 8675, pp.281-288. Springer, Cham (2023). https://doi.org/10.1007/978-3-319-10443-0_36
28. Cheng, J., Shen, D., Yap, P. T., et al.: Single-and multiple-shell uniform sampling schemes for diffusion MRI using spherical codes. *IEEE transactions on medical imaging* **37**(1), 185-199 (2017)
29. Daducci, A., Canales-Rodríguez, E. J., Zhang, H., et al.: Accelerated microstructure imaging via convex optimization (AMICO) from diffusion MRI data. *Neuroimage* **105**, 32-44 (2015)
30. Park, J., Jung, W., Choi, E. J., et al.: DIFFnet: diffusion parameter mapping network generalized for input diffusion gradient schemes and b-value. *IEEE Transactions on Medical Imaging* **41**(2), 491-499 (2021)